High temperature polymer foams

J. Hedrick*, J. Labadie, T. Russell, D. Hofer and V. Wakharker
IBM Research Division, Almaden Research Center, 650 Harry Road, San Jose, CA 95120-6099, USA
(Received 29 September 1992; revised 23 February 1993)

A means of generating high temperature polymer foams with pore sizes in the nanometre range has been developed. Foams were prepared by casting block copolymers comprising a thermally stable block as the matrix and a thermally labile material as the dispersed phase. Upon thermal treatment the thermally unstable block underwent thermolysis, leaving pores with a size and shape dictated by the initial copolymer morphology. Nanopore foam formation is shown for triblock copolymers composed of a poly(phenylquinoxaline) (PPQ) matrix with either poly(propylene oxide) (PO) or poly(methyl methacrylate) (PMMA) as the thermally labile coblocks. Upon decomposition of these blocks, a 10–20% reduction in density was observed, consistent with the initial PO or PMMA composition, and the resulting PPQ foams showed dielectric constants of about 2.4, substantially lower than that of PPQ (2.8). Small-angle X-ray scattering and transmission electron microscopy showed pore sizes of approximately 100 Å.

(Keywords: foams; pores; copolymers)

INTRODUCTION

High performance polymers play an important role as packaging materials in the manufacture of microelectronic devices and components, and are finding applications as interlayer dielectrics for thin film wiring in multichip packages and chip interconnection. Material requirements generally include high thermal stability, low thermal expansion and residual stress from thermal cycling, and good mechanical properties. Since the velocity of pulse propagation is inversely proportional to the square root of the dielectric constant of the medium, a reduction in the dielectric constant of the insulating material translates directly into improvements in machine cycle time[1]. Also, the minimum distance between lines is dictated by noise arising from current induced in conductors adjacent to active signal lines. This 'crosstalk' depends upon the dielectric constant of the insulating material[1]. Therefore a reduction in the dielectric constant of the insulator allows the signal lines to be closer.

As a class of materials, polyimides have best satisfied the material requirements for these applications. The aromatic polyimide derived from pyromellitic dianhydride (PMDA) and 4,4′-oxydianiline (ODA) has received the most attention in the microelectronics industry due to its availability, ease of processing, solvent resistance and excellent mechanical properties. These latter two properties can be attributed, in part, to the ordering of the polymer and the alignment of chains parallel to the surface[2,3]. The ordering, however, can cause poor planarization and self-adhesion, whereas the molecular orientation results in an anisotropic dielectric constant[4] with a higher dielectric constant parallel to the film surface. This substantially reduces the advantage gained over inorganic materials by polymers.

The most common approach in modifying the dielectric properties of polyimides has been via the incorporation of perfluoroalkyl groups. Examples include the incorporation of hexafluoroisopropylidene linkages (Hoechst Sixef)[5], main chain perfluoroalkylene groups[6] and pendant trifluoromethyl groups[7,8]. This approach produces films with dielectric constants below 3.0 (as low as 2.6 for Hoechst Sixef) and low water absorption ($\sim 0.5\%$); however, the mechanical properties are sacrificed. The addition of pendant trifluoromethyl groups appears to circumvent this drawback, but the incorporation of sufficient trifluoromethyl groups into the polymer is limited synthetically. An alternative strategy involves the introduction of a low dielectric polymer as a distinct phase in a rigid polyimide matrix. A block copolymer approach has been investigated for PMDA/ODA, using a perfluoroalkylene aryl ether as the coblock[9]. Incorporation of the fluorinated coblock reduced the dielectric constant from 3.1 to 2.8, and decreased the moisture uptake without significant compromise to the thermal and mechanical properties. A more significant reduction in dielectric constant by this approach requires functional oligomers derived from lower dielectric constant polymers, which would be difficult to prepare and copolymerize.

One alternative to the above procedures is to generate a polyimide foam. The reduction in the dielectric constant is simply achieved by replacing the polymer, having a dielectric constant of about 3.2, by air with a dielectric constant of 1. Thus a film containing 25% voids will have a dielectric constant of about 2.65. However, the size of the pores or voids is critical; it is essential that the size of the voids should be much smaller than the film thickness and any microelectronic features. Secondly, the voids or pores must be closed-cell to retard the penetration of solvent during subsequent processing, and

* To whom correspondence should be addressed

0032-3861/93/224717-10

the foam must be stable under typical conditions of fabrication and use.

Polyimide foams have been developed primarily for use in the aerospace and transportation industries[10]. The routes to the preparation of polyimide foams include the use of foaming agents[11–13], partial degradation generating a foaming agent[14–22], the inclusion of glass or carbon microspheres[23–27] and microwave processing[28].

The synthesis and properties of a foamed poly(phenylquinoxaline) (PPQ) are reported here. The foam is prepared by the synthesis of a PPQ copolymer, in which one polymer block undergoes thermal decomposition to volatile products. This concept is similar to that developed by Patel *et al.*[29] for the preparation of epoxy networks with well-defined microporosity. However, rather than using the phase separation of two polymers, which leads to phase separation on the micrometre scale, the work described here takes advantage of the small size scale of microphase separation inherent to block copolymers. Here, the thermall unstable block comprises the minor phase embedded in a PPQ matrix. Upon degradation of the unstable block, voids are left in the PPQ matrix, with a size commensurate with the microphase separated block copolymer morphology, i.e. on the scale of the radius of gyration of the minor components. Thus, the term 'nanofoam' is used. By adjusting the molecular weights of the two components, the volume fraction and size of the resultant voids can be varied. For the experiments reported in this article, triblock copolymers of PPQ with either poly(propylene oxide) (PO) or poly(methyl methacrylate) (PMMA) were used, where the latter polymers undergo thermolysis to volatile products and hence are easily removed.

EXPERIMENTAL

Materials

Bis(phenylglyoxalyl)benzene (BPGB), 3,3′-diaminobenzidine (DAB) and 4-hydroxybenzil were obtained and purified as described previously[30]. Monofunctional PO oligomers with $\bar{M}_n$ of 5000 and 10 000 g mol^{-1} were kindly provided by Dow Chemical and were kept *in vacuo* prior to use. A 1.9 M phosgene/toluene solution was obtained from Fluka and was used as received. Group transfer polymerized PMMA with $\bar{M}_n = 15\,000$ g mol^{-1} was kindly supplied by DuPont.

Benzil end-capped PO oligomers

The general method for functionalization of PO oligomers with a benzil end group is given for the oligomer with $\bar{M}_n = 5000$. A 100 ml three-neck round-bottom flask fitted with a dry-ice condenser and a nitrogen inlet was charged with 10.0 g (2.00 mmol) of PO followed by 25 ml (50 mmol) of phosgene/toluene solution. The stirred mixture was heated to 60°C for 2 h in a water bath. The phosgene and toluene were removed with a strong stream of nitrogen, followed by evacuation for several hours. The resulting viscous oil was diluted with 50 ml of methylene chloride and 430 mg (1.90 mmol) of 4-hydroxybenzil was added. The mixture was cooled to 0°C and 5 ml of pyridine was added dropwise. The reaction mixture was allowed to warm to room temperature overnight and then partitioned between methylene chloride and 5% aqueous HCl. The organic layer was separated and washed twice with 5% aqueous HCl and water, and dried with magnesium sulfate. Concentration of the organic extract on a rotary evaporator, followed by pumping for 18 h at 0.1 mmHg yielded 8.2 g of the desired oligomer as a clear oil. Comparison of the benzil and PO backbone spectral resonances by ^{1}H n.m.r. showed the oligomer to have $\bar{M}_n = 6000$ g mol^{-1} (referred to as 6K PO).

The PO oligomer with $\bar{M}_n = 10\,000$ was prepared by the same general procedure using 10 g (1 mmol) of monofunctional hydroxy end-capped PO, 25 ml of phosgene/toluene, 215 mg (0.95 mmol) of hydroxybenzil, 2.5 ml pyridine and 50 ml of chloroform. Analysis by ^{1}H n.m.r. showed the oligomer to have $\bar{M}_n = 9400$ g mol^{-1} (referred to as 9.4 K PO).

Benzil end-capped PMMA oligomers

The method of functionalization of the PMMA oligomer was analogous to that of the PO oligomers and is described for the PMMA oligomer with $\bar{M}_n = 15\,000$. A three-neck 500 ml flask equipped with a mechanical stirrer and a dry-ice condenser was charged with 50 ml of chloroform and warmed to 40°C. The PMMA oligomer (20.0 g, 1.33 mmol) was added in portions to the stirred chloroform. An additional 5 ml of chloroform was used to rinse the PMMA from the walls of the flask. After dissolution of the PMMA, 15 ml of 20% phosgene/toluene solution (3.0 g, 30 mmol phosgene) was added. The reaction mixture was warmed to 55°C and held for 2 h. The heating was discontinued and the excess phosgene was removed by passing a strong flow of nitrogen over the solution for 18 h. The resulting glass was evacuated under reduced pressure for 2 h, broken up with a spatula and evacuated under reduced pressure for an additional 2 h. To the glassy solid was added 200 ml of chloroform and 300 mg (1.33 mmol) of 4-hydroxybenzil. The solution was cooled in an ice-bath and treated with 5.0 ml of pyridine. The reaction was warmed to room temperature, stirred for several hours and precipitated in methanol. The resulting powder was further washed with water and twice with methanol. The white powder was dried *in vacuo* to constant weight, affording 19.0 g of oligomer. Comparison of the integration of the aromatic benzil and aliphatic PMMA resonances by ^{1}H n.m.r. showed the oligomer to have $\bar{M}_n = 15\,000$ g mol^{-1} (referred to as 15 K PMMA).

PPQ–PO block copolymers

Block copolymers were prepared under conditions analogous to those for conventional PPQ synthesis. A copolymer with a theoretical composition of 20% 6 K PO was synthesized by slurring 7.1517 g (33.377 mmol) of DAB in 40 ml of *m*-cresol/xylene (1:1). A solution of 11.313 g (33.050 mmol) of BPGB and 4.00 g (0.66 mmol) of the benzil end-capped oligomer in 100 ml of *m*-cresol/xylene was added dropwise to the slurry with stirring. When the addition was complete, the addition funnel was rinsed with 30 ml of *m*-cresol/xylene and the polymerization mixture was stirred for 20 h. The polymer was isolated by precipitation in methanol followed by three methanol washes. The copolymer was isolated in 88% yield. Analysis of the copolymer by ^{1}H n.m.r. showed 13.4 wt% PO composition by integration of aromatic PPQ resonances *versus* the PO resonances. The analogous copolymer based on the 9.4 K oligomer was isolated in 90% yield and had a PO composition of 16.5 wt%.

PPQ–PMMA block copolymers

The PPQ–PMMA block copolymers were prepared in an analogous fashion to those described above. A copolymer with a 35 wt% theoretical composition of the 15 K PMMA oligomer was synthesized by slurring 2.300 (0.0107 mol) of DAB in 40 ml of *m*-cresol. A solution of 3.6397 g (0.010642 mol) of BPGB and 3.1500 g (0.000021 mol) of PMMA oligomer dissolved in 20 ml *m*-cresol was added dropwise to the slurry with stirring. It is important to note that xylene was not used as a constant since it interfered with the solvation of the PMMA. When the addition was complete, the addition funnel was rinsed with 20 ml of *m*-cresol and stirred for 20 h. The polymerization was isolated by precipitation in methanol followed by two additional methanol rinses and one rinse in tetrahydrofuran.

Foam formation

The copolymers were dissolved in tetrachloroethane (TCE) at a concentration of 9% solids. Coatings of 10 μm thickness were obtained by spin coating at 2000 rev min^{-1} on Si wafers, 2.54 cm in diameter. The solvent TCE was removed by heating the polymer films to 150°C at 5°C min^{-1} and maintaining them at 150°C for 2 h in a nitrogen atmosphere. The films were then cooled to room temperature and reheated to 275°C at a rate of 5°C min^{-1} and maintained at 275°C for 9 h in air.

Measurements

Dielectric measurements on the polymer films were carried out using an HP multifrequency analyser. Medium frequency (10 kHz–4 MHz) capacitance and loss tangents were measured in the temperature range 25–100°C. Specimens for the dielectric measurements were prepared by vacuum deposition of gold electrodes, 3 mm in diameter, on the spin-coated polymer films with the back surface of the Si wafer serving as the other electrode. Glass transition temperatures, taken as the midpoint of the change in slope of the baseline, were measured on a DuPont DSC 1090 instrument with a heating rate of 10°C min^{-1}. The dynamic mechanical measurements were performed on a Polymer Laboratories dynamic mechanical thermal analyser at 10 Hz with a heating rate of 10°C min^{-1} in the tension mode. Isothermal and variable temperature (5°C min^{-1} heating rate) thermal gravimetric analysis (t.g.a.) measurements were performed on a Perkin–Elmer model TGA-7 in a nitrogen atmosphere. Density measurements were obtained with a density gradient column made from carbon tetrachloride and xylene. The column was calibrated against a set of beads of known densities at 25°C. At least three specimens were used for each density measurement. Small-angle X-ray scattering (SAXS) measurements were performed on a Kratky camera using a 60 μm entrance slit with Ni filtered Cu radiation from a Rigaku 18 kW rotating anode generator operated at 100 kV and 40 mA.

RESULTS AND DISCUSSION

PPQ was chosen as the matrix due to its thermal stability, high glass transition temperature, T_g, and good processability[31–33]. PPQ is amorphous and thin films have been shown to be isotropic, which can be important for foam stability. It is also soluble in the fully cyclized form, thus eliminating curing steps which contribute to film shrinkage and stress. PPQ also has low moisture uptake (<0.1 wt%) and permeability, which is critical for maintaining a low dielectric constant. PPQ in itself has a dielectric constant of 2.8, which is low in comparison to other high temperature polymers.

The criteria for the thermally decomposable coblock include the synthesis of well-defined functional oligomers, compared with the synthesis of PPQ. This block must also decompose quantitatively into non-reactive species that can easily diffuse through a glassy PPQ matrix. The temperature at which decomposition occurs is critical: it should be sufficiently high to permit standard film preparation and solvent removal below the T_g of the PPQ block to avoid foam collapse. Two thermally laile polymers were investigated: PO and PMMA. Each decomposes quantitatively between 275 and 350°C to small molecules, which should readily diffuse through the high temperature polymer matrix. PO is stable in an inert atmosphere up to 300°C. However, when exposed to oxygen, PO decomposes rapidly between 250 and 300°C. *Figure 1* shows the t.g.a. thermogram of PO heated isothermally at 275°C in air. Within 20 min a quantitative decomposition is observed. The thermal decomposition temperature of PMMA is strongly dependent on the polymerization mechanism used, since the degradation

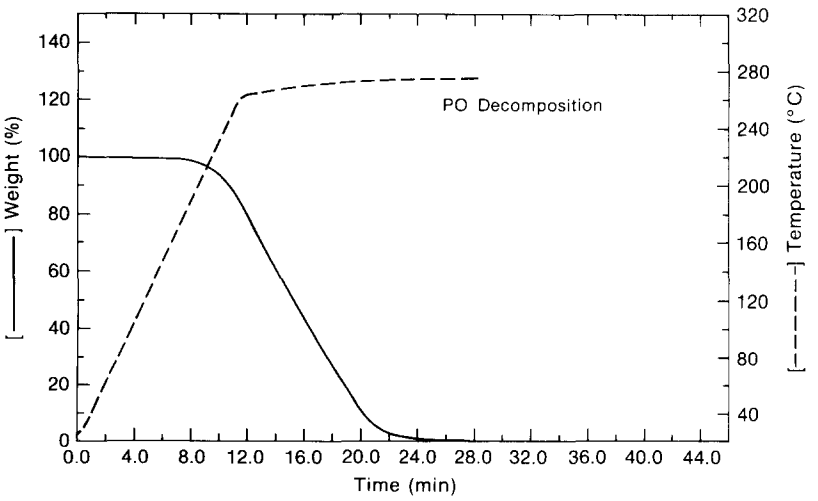

Figure 1 Thermogravimetric analysis of PO

occurs via a depolymerization process. For example, PMMA prepared by free radical methods produces a substantial amount of chain ends terminated via a disproportion reaction. Typically, such PMMA degrades at relatively low temperatures. Conversely, PMMA prepared by anionic or group transfer methods has well-defined end groups and substantially higher decomposition temperatures. In fact, the PMMA used in this study has a decomposition temperature of 335°C, as shown in *Figure 2*. However, when converted to the benzil derivative, the alphatic carbonate linkage reduces the thermal stability of the PMMA markedly, as shown in *Figure 2*. This is critical for the generation of the nanofoam since 335°C is close to the T_g of PPQ. The characteristics of the oligomers are shown in *Table 1*.

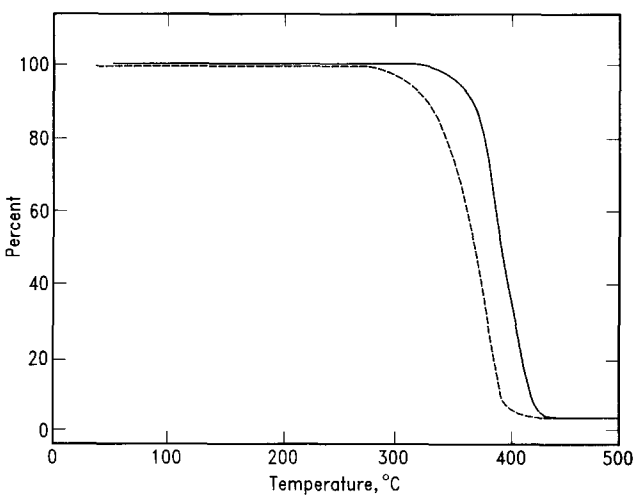

Figure 2 Thermogravimetric analysis of PMMA (——) and benzil end-capped PMMA (----)

Table 1 Characteristics of propylene oxide and methyl methacrylate oligomers

Oligomer type	$\bar{M}_n$ (g mol^{-1})	T_g (°C)
PO	6000	−71
PO	9400	−72
PMMA	15000	115

The synthetic schemes used for the preparation of the PPQ–PO and PPQ–PMMA triblock copolymers were based on a monomer/oligomer synthetic approach (*Scheme 1*). It has been shown that phenolic hydroxyl-terminated PPQ oligomers of controlled molecular weight can be synthesized by the co-addition of a mixture of BPGB and 4-hydroxybenzil to a slurry of DAB in an *m*-cresol/xylene (50/50) solvent mixture[33]. By analogy, the desired triblock copolymers were prepared by the addition of a mixture of BPGB and either the benzil end-capped PO or PMMA oligomer to a solution of DAB. The use of the monofunctional oligomers serves to cap the chain ends producing an ABA block architecture, where either the PO or PMMA comprise the end or A blocks. For the PPQ–PO triblock synthesis, a xylene/*m*-cresol (50/50) solvent mixture, typical for PPQ syntheses, was used as the polymerization medium. However, for the PPQ–PMMA copolymerization, *m*-cresol was used exclusively as the solvent to avoid cloudy solutions. During the initial stages of the polymerization, the DAB was not soluble in the solvents. However, upon addition of the BPGB and the benzil end-capped oligomers, the polymerizations proceeded similarly to PPQ syntheses, yielding clear red–brown solutions of moderate viscosity. It is important to note that the stoichiometric offset between BPGB and DAB is minimal ($\ll 0.5\%$), since the oligomers used are monofunctional and have such high molecular weight. Thus, the molecular weight of the PPQ block is high, and after foam formation the remaining PPQ should have excellent mechanical properties. The copolymers were precipitated in methanol and rinsed several times to remove unreacted PO or PMMA and residual *m*-cresol. The yield of the isolated copolymers was approximately 90%.

Several triblock copolymers were prepared with PO and PMMA compositions varying from approximately 20 to 35 wt%. Compositions were deliberately maintained low so as to maximize the possibility of having discrete, non-continuous domains of either PO or PMMA in a PPQ matrix. This was done to facilitate the formation of a stable foam upon decomposition of the thermally labile block. The copolymer compositions were varied by adjusting the stoichiometry of the components according to Carother's equation (*Table 2*). The copolymer composition was determined using both ^{1}H n.m.r., by comparison of the integrated PPQ signal

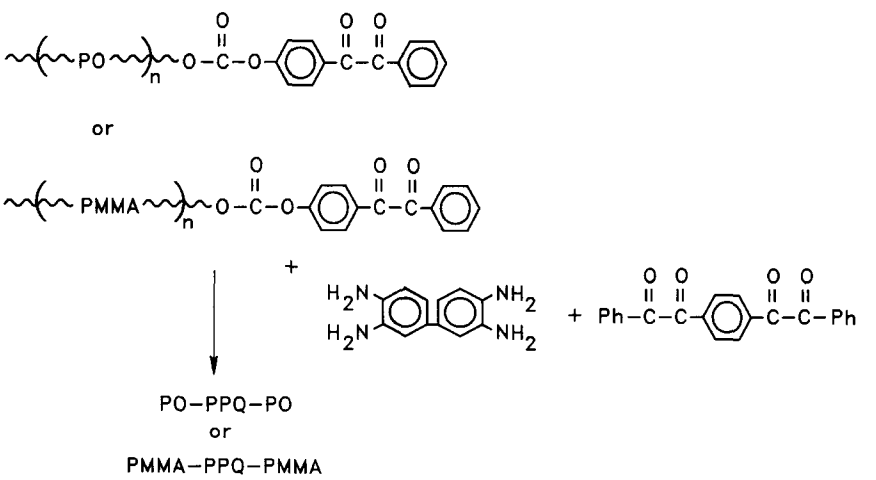

Scheme 1

Table 2 Characteristics of phenylquinoxaline–propylene oxide and phenylquinoxaline–methyl methacrylate triblock copolymers

Copolymer number	Coblock type	Coblock mol. wt ($g\,mol^{-1}$)	Composition of coblock (wt%)			Volume fraction (%)	T_g of copolymers (°C)	
			Theoretical	N.m.r.	T.g.a.		Coblock	PPQ
1	PO	6000	20	13.4	14.0	17	−40	360
2	PO	6000	30	21.0	22.0	27	−45	360
3	PO	9400	20	16.5	16.0	20	−42	361
4	PO	9400	30	24.0	24.0	31	−47	360
5	PMMA	15000	20	–	17.0	–	–[a]	360
6	PMMA	15000	35	–	27.0	–	–[a]	360

[a] Not detectable by d.s.c.

to that of either the PO or PMMA resonances, and by t.g.a., by measuring the weight retention after the decomposition of the thermally labile block. The PO compositions for the triblock copolymers derived from the 6K PO oligomer were 13.4 and 21 wt% for copolymers 1 and 2 (see *Table 2*), respectively, while the triblock copolymers derived from the $9400\,g\,mol^{-1}$ oligomer were 16.5 and 24% for copolymers 3 and 4, respectively. The composition of PMMA in the triblock copolymers was 17 and 27 wt% for copolymers 5 and 6, respectively, as shown in *Table 2*. *Table 2* also contains the volume fractions of either PO or PMMA in the copolymers, based on the densities of $1.028\,g\,cm^{-3}$ for PO, $1.15\,g\,cm^{-3}$ for PMMA and $1.32\,g\,cm^{-3}$ for PPQ. The composition of PO and PMMA incorporated in the copolymers is somewhat lower than that charged, owing to the solvent rinses which remove homopolymer contamination as well as copolymers rich in PO or PMMA. For all the copolymers prepared, the theoretical $\bar{M}_n$ of the PPQ block, as determined by the stoichiometric offset used in the synthesis, exceeded $50\,000\,g\,mol^{-1}$. Due to the high PPQ block length required to give triblock copolymer, it is likely that some diblock copolymer may exist.

A key component in generating a nanofoam is the ability to process the block copolymer precursor by conventional methods. The PO and PMMA decomposition temperatures are high enough to allow removal of common solvents prior to void formation, and after solvent removal the thermally labile block can be decomposed with a subsequent heat treatment. The copolymers were dissolved in TCE and spun into thin films ($\sim 10\,\mu m$). The films were then heated to 150°C for 2 h to remove the solvent. Isothermal gravimetric analysis under identical conditions indicated that virtually no degradation of either the PO or PMMA had occurred during this step. For the case of the PPQ–PO copolymers, two T_gs were observed at about −40 and 360°C (*Table 2*), indicative of a microphase separated morphology. The T_g of the PO in the copolymer was somewhat higher than the initial oligomer, suggesting at least a partial phase mixing in this domain. Conversely, the PPQ transition in the copolymer was identical to that of the homopolymer, consistent with the high molecular weight of this block. The dynamic mechanical measurements, consistent with calorimetry results, show two transitions. The low temperature regimes for the two copolymers are shown in *Figure 3*. The PO transition in the copolymer is broad, indicative of a diffuse phase boundary. Likewise, the PPQ–PMMA copolymers

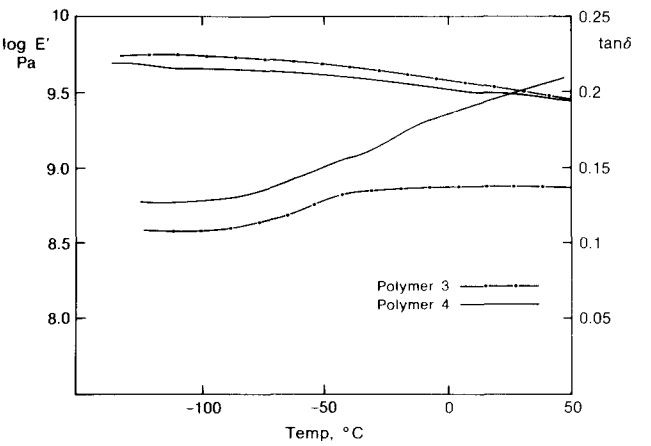

Figure 3 Dynamic mechanical behaviour of PPQ–PO copolymers 3 and 4

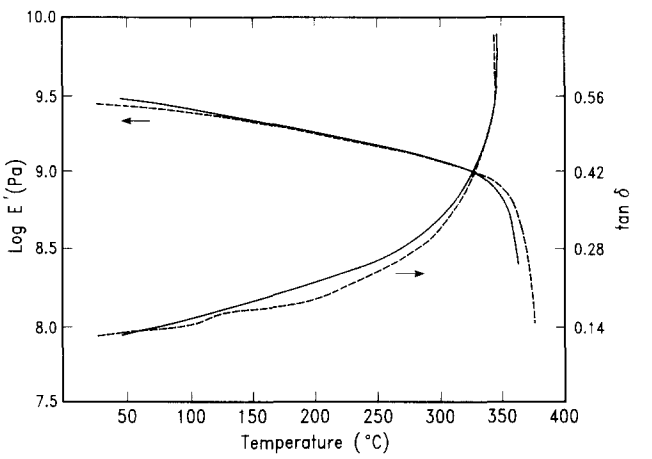

Figure 4 Dynamic mechanical behaviour of PPQ–PMMA copolymers 5 (——) and 6 (– – – –)

showed two transitions by calorimetric (*Table 1*) and dynamic mechanical (*Figure 4*) analyses. The PMMA transition is only slightly higher than the parent oligomer, while the PPQ transition is identical to that of the homopolymer. Although the PMMA block has a narrow molecular weight distribution, the high degree of phase purity was surprising, since it is difficult to attain heterogeneous morphologies in many glassy–glassy high temperature polymers.

The generation of the nanofoam structure was accomplished by a subsequent heat treatment of the triblock polymers to decompose the thermally labile block. It is important that the decomposition products,

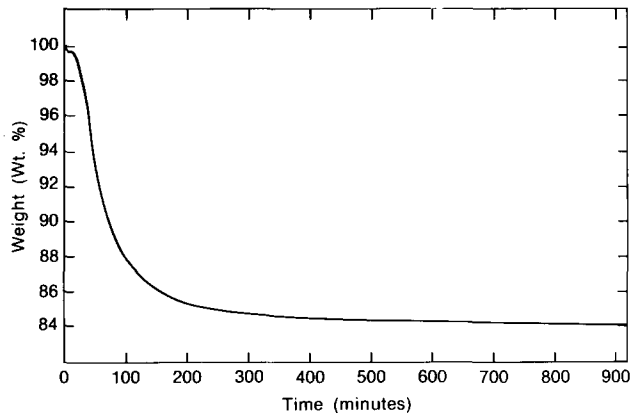

Figure 5 Thermogravimetric analysis of PPQ–PO copolymer 3 at 275°C in air

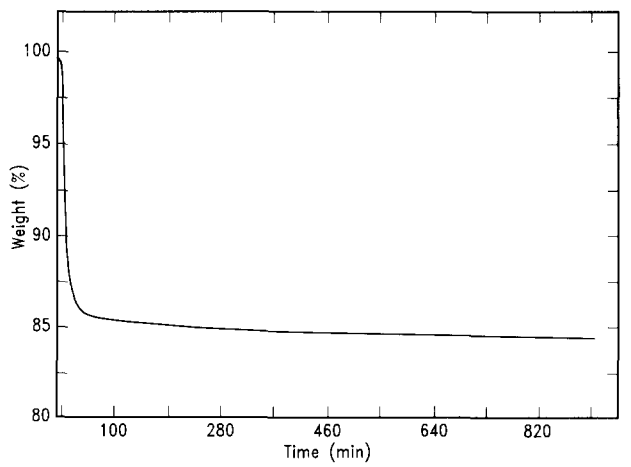

Figure 6 Thermogravimetric analysis of PPQ–PMMA copolymer 5 at 340°C in air

which include possible radical species, do not react with the polymer matrix since this would be detrimental to the resulting dielectric constant. For the case of the PPQ–PO triblock polymers, the films were heated to 275°C (9 h) in air to thermally decompose the PO. Isothermal gravimetric analysis indicated that the decomposition of the PO in the copolymer was complete under these conditions (*Figure 5*). The PPQ–PMMA copolymers required substantially higher temperatures to decompose the PMMA block. The films were heated to 340°C (5 h) in air to decompose thermally the PMMA block, and isothermal gravimetric analysis showed that the decomposition of the PMMA was complete under these conditions (*Figure 6*). These data indicate that the *in situ* decomposition of either the PO or PMMA was quantitative, with no evidence of side reactions and with complete elimination of the labile component.

The density of the polymer clearly shows the formation of a foamed polymer. The density values of the foamed copolymers 1–6 are shown in *Table 3*, together with PPQ homopolymer. For the PPQ, the density was 1.32 g cm^{-3}, while the copolymers showed substantially lower values. The densities of the copolymers ranged from 1.17 to 1.19 g cm^{-3}, which is approximately 88–90% of that of PPQ. This is consistent with 10–12% of the film being occupied by voids. Furthermore, the foam structure appears to be stable over a wide temperature range. *Figure 7* shows the densities of PPQ and copolymer 3 as a function of the processing temperature. For the PPQ, the density was essentially independent of process temperature. Copolymer 1, on the other hand, underwent substantial changes. After drying at 150°C the density was 1.29 g cm^{-3}, consistent with the volume additivity of the PO and PPQ blocks. After heating to 200°C, the density dropped to 1.17 g cm^{-3}, which suggests the formation of a foam. The density remained at this value up to about 350°C, whereupon the density began to increase. At 400°C, the density approached that of PPQ indicating that the foam structure had collapsed. However, the foam structure was maintained over a large temperature range.

While the density showed that the generation of a foam had been successfully achieved, no information was provided on the size of the pores. To address this issue, both transmission electron microscopy (TEM) and SAXS were used. *Figure 8* shows the TEM of a typical microtomed section of copolymer 3 after decomposition of the PO block. The dark regions in the micrograph correspond to the PPQ matrix. From the micrograph it is evident that a porous structure is obtained, with pores having an average diameter of 8–10 nm. It is also clear that little interconnectivity between the pores and the desired morphology has been achieved. However, it is difficult to interpret the micrographs quantitatively because the specimens must be microtomed, which could distort the morphology, and the thin sections are comparable in thickness to the size of the pores. Consequently, partial transmission of the electron beam occurs, giving rise to an apparently large volume fraction of pores. In fact, the fraction of pores in the micrograph appears to be much greater than the expected 12%. However, the porous nature of the films is unequivocal.

SAXS, on the other hand, offers an alternative means of addressing this issue. *Figure 9* shows a series of SAXS profiles for PPQ, copolymer 3 and the copolymer after decomposition of the PO block. The data are plotted as

Table 3 Density measurements of poly(phenylquinoxaline) and foamed copolymers

Copolymer number	Density (g cm^{-3})
PPQ	1.32
1	1.17
2	1.18
3	1.16
4	1.19
5	1.18
6	1.19

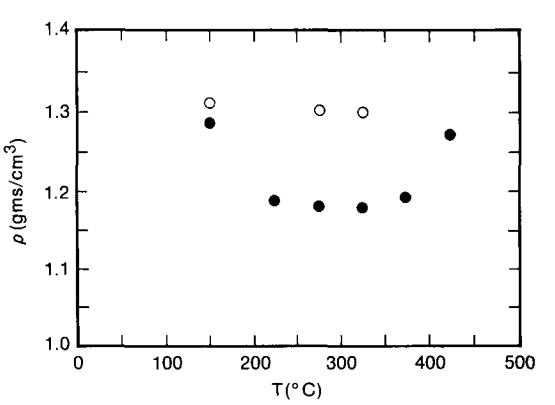

Figure 7 Density measurements as a function of temperature for PPQ (○) and foamed copolymer 3 (●)

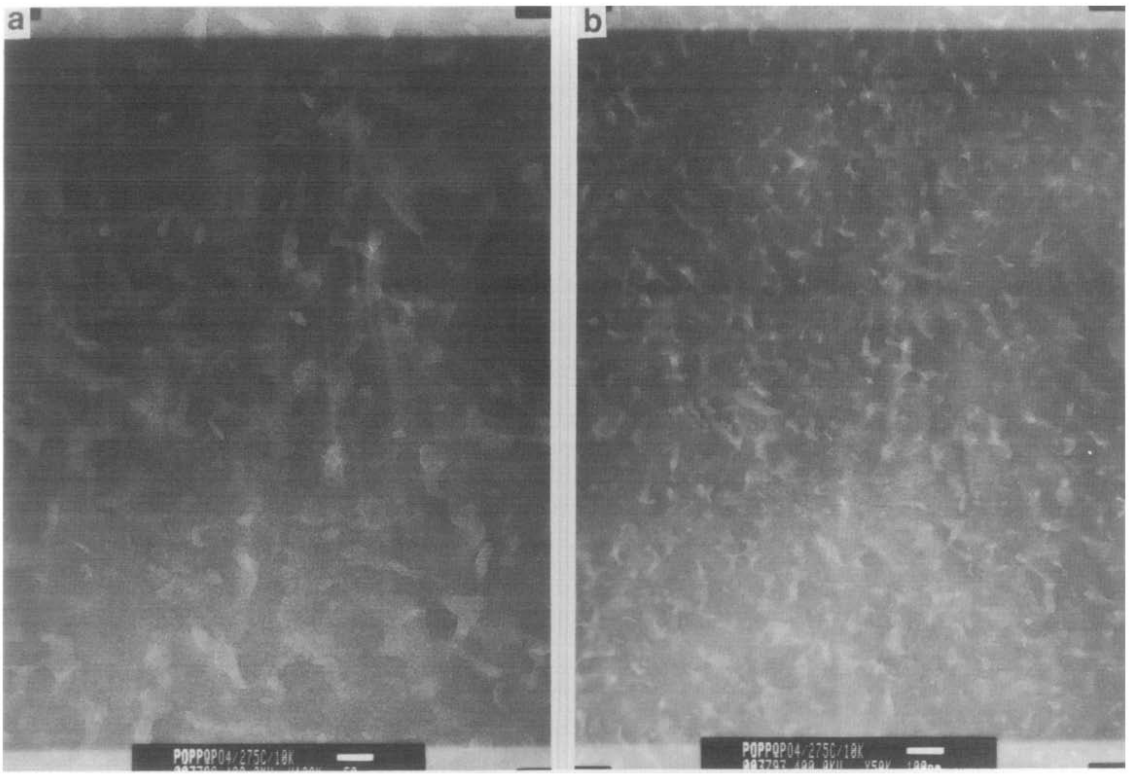

Figure 8 TEM micrograph of foamed copolymer 3: (a) 100 000 ×; (b) 50 000 ×

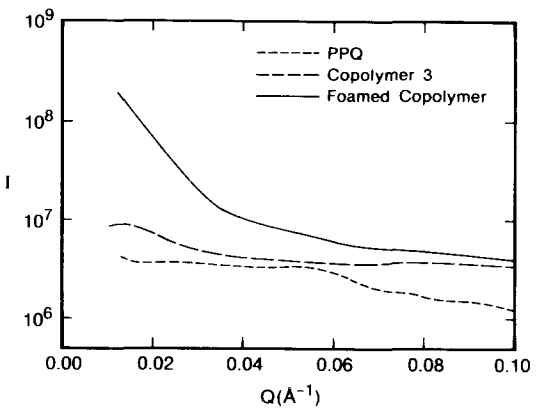

Figure 9 SAXS profiles for PPQ, copolymer 3 and foamed copolymer 3

the logarithm of the scattering as a function of the scattering vector, $Q=(4\pi/\lambda)\sin\theta$, where λ is the wavelength (1.542 Å) and 2θ is the scattering angle. The scattering arising from the PPQ and copolymer 3 is weak. Any angular dependence of the scattering at high Q can be attributed to the weak nature of the scattering and the difficulty associated with proper subtraction of the background. The copolymer shows a slight increase in the scattering at low Q which can be attributed to the two-phase nature of the copolymer. The weakness of this scattering arises from the low contrast between the PPQ and PO phases. Upon decomposition of the PO block, an increase in the scattering of more than an order of magnitude occurs. This is consistent with decomposition and removal of the PO, forming a void. The large electron density difference between the pores and the matrix produces the dramatic increase in scattering.

From the angular dependence of the scattering, a measure of the size of the pores can be obtained. The type of morphology being dealt with is the classic structure studied by Debye and co-workers[34,35], where one has a dense, two-phase system with sharp phase boundaries. Here, the matrix is a glass and the second phase is void. The correlation length, a, defines the average size of heterogeneities in a system and the observed scattering is given by:

$$I(q)=i_e V\overline{(\Delta\rho)^2}\int_0^\infty \gamma(r)4\pi r^2 \sin qr\, dr \qquad (1)$$

where $\gamma(r)$ is the correlation function at a distance r, i_e is the Thomson scattering factor, $\overline{(\Delta\rho)^2}$ is the mean square electron density difference and V is the scattering volume. For a random two-phase system $\gamma(r)$ can be approximated by $e^{-r/a}$ which, upon substitution, gives:

$$I(q)=i_e V\overline{(\Delta\rho)^2}\left[\frac{(8\pi^3)}{(1+q^2a^2)^2}\right] \qquad (2)$$

Thus, a plot of $I(q)^{-1/2}$ *versus* q^2 yields the correlation length from the ratio of the slope to the intercept. Similar arguments can be given for slit smeared data, which is of interest here. The correlation length, as shown by Kratky[36], is related to the average chord length or dimension of the phases by:

$$l_1=\frac{a}{\phi_2} \quad \text{and} \quad l_2=\frac{a}{\phi_1} \qquad (3)$$

where l_i is the chord length of phase i with volume fraction ϕ_i.

For the PO–PPQ–PO triblock copolymer, after decomposition of the PO block, this analysis yielded the data shown in *Table 4*. Assuming that the volume fraction of polymer in the foam is given by the ratio of the density of the foamed copolymer divided by that of the PPQ, then correlation lengths of 8–9 nm are obtained, which translates into chord lengths or average pore sizes of

Table 4 Characteristics of poly(phenylquinoxaline) nanofoams

Sample	ϕ_v[a]	Density (g cm^{-3})	a[b] (nm)	l_p[c] (nm)
PPQ	–	1.32	–	–
Polymer 3	12.0	1.16	7.0	8.0
Polymer 4	9.8	1.19	8.1	8.8
Polymer 5	11.5	1.18	7.5	8.4
Polymer 6	9.0	1.19	6.9	7.6

[a] ϕ_v is the volume fraction of pores
[b] a is the correlation length
[c] l_p is the average dimension of the pores or chord length of the pores

Table 5 Dielectric properties of high temperature polymer foams

Copolymer number	Temperature (°C)	Frequency (kHz)	Dielectric constant
3	45	20	2.38
	45	2×10^3	2.31
	100	20	2.36
	100	2×10^3	2.31
4	45	20	2.55
	45	2×10^3	2.51
	100	20	2.54
	100	2×10^3	2.50
PPQ	45	20	2.86
	45	2×10^3	2.70
	100	20	3.05
	100	2×10^3	2.82

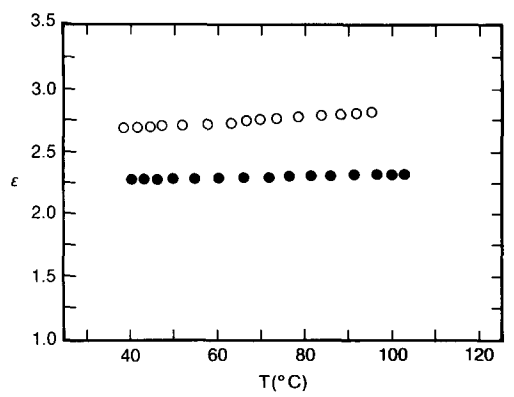

Figure 10 Dielectric constant of PPQ (○) and foamed copolymer 3 (●) as a function of temperature

8–8.9 nm. This is consistent with the TEM results shown previously, and demonstrates the formation of pores on the scale of tens of nanometres.

The results obtained from the dielectric measurements are shown in *Table 5*. The dielectric constant for the foamed copolymer 3 was 2.31 while that for the PPQ under similar conditions was 2.70. This is nearly a 15% reduction in the dielectric constant. However, it is interesting to note that the foam of copolymer 4 has a slightly higher dielectric constant (2.51) even though the composition of PO incorporated was higher (*Table 3*). These data are consistent with both the density and SAXS measurements and will be discussed later in the text. *Figure 10* shows the dielectric constant of PPQ and the foam of copolymer 3 as a function of temperature. As expected, for PPQ the dielectric constant was 2.7, essentially independent of temperature. For the foamed copolymer 3 the dielectric constant was invariant up to temperatures in excess of 100°C, indicating no water uptake. This was not unexpected since both water absorption and permeability of water are minimal in PPQ.

An important factor in these studies is the variation in the dielectric constant with the volume fraction of voids. From the electron micrographs it appears that a reasonable model for the nanofoams would be essentially that for a composite material where the dispersed component, in this case, is spherical voids with a distribution of sizes. The Maxwell–Garnett model, used for the calculation of the dielectric constant of composites, assumes a random arrangement of spheres of uniform size having an isotropic polarizability. The results from this calculation are shown in *Figure 11*. As can be seen, the model calculation does not agree with that observed for the PPQ foams (indicated by the solid circle). It is unlikely that the incorporation of a distribution of sphere sizes would improve the agreement between the calculation and the observed dielectric constant. Alternatively, a simple additivity of the dielectric constant could be assumed where $\varepsilon = \phi_{PPQ}\varepsilon_{PPQ} + \phi_v\varepsilon_v$. As with the Maxwell–Garnett model, the calculation disagrees with the data. Empirically, the best agreement with the experimental data was found when it was assumed that $1/\varepsilon = (\phi_{PPQ}/\varepsilon_{PPQ}) + (\phi_v/\varepsilon_v)$. While, with only limited data, the agreement between the calculated and observed dielectric constant does not consitute proof that this empirical relation describes the entire concentration dependence of ε, it does indicate that a simple volume additivity of the dielectric constants of the components does not describe the observation.

It should be noted that the volume fraction of voids does not correspond to the volume fraction of the PO or PMMA in the parent copolymer. For the lower PO or PMMA contents, this can be understood by realizing that there is a distribution in the sizes of the PO or PMMA microphases. In fact, a small fraction of PO or PMMA will be dispersed in the PPQ. Upon decomposition of the PO or PMMA, the smallest voids will collapse simply due to a surface pressure, whereas the larger ones will remain. While this provides a convenient explanation for the slight differences in the expected and observed volume fractions for the low PO or PMMA content copolymers, this does not apply to the higher content copolymers, where the discrepancies are much larger. Here, however, at volume fractions approaching 0.3, the morphology will no longer consist of isolated PO or PMMA domains in a PPQ matrix. Rather, there will be much more interconnectivity. This interconnectivity must destabilize the PPQ matrix, causing a large-scale collapse of the foam. Consequently, this observation leads to the conclusion that there is a maximum volume fraction of voids that can be incorporated into the polymer using this approach.

One major concern in generating a foam by this approach is whether the cellular structure, having a very high surface area prone to collapse, would be retained over repetitive thermal cycles. Furthermore, one can envision the voids as stress concentrators, possibly initiating such deformation processes as stress relaxation, crazing or plastic deformation with the development of thermal stresses. The deformation process is directly related to the polymer structure; however, the former, in particular, may lead to the collapse of the foam. The stress from thermal cycling is directly related to both the

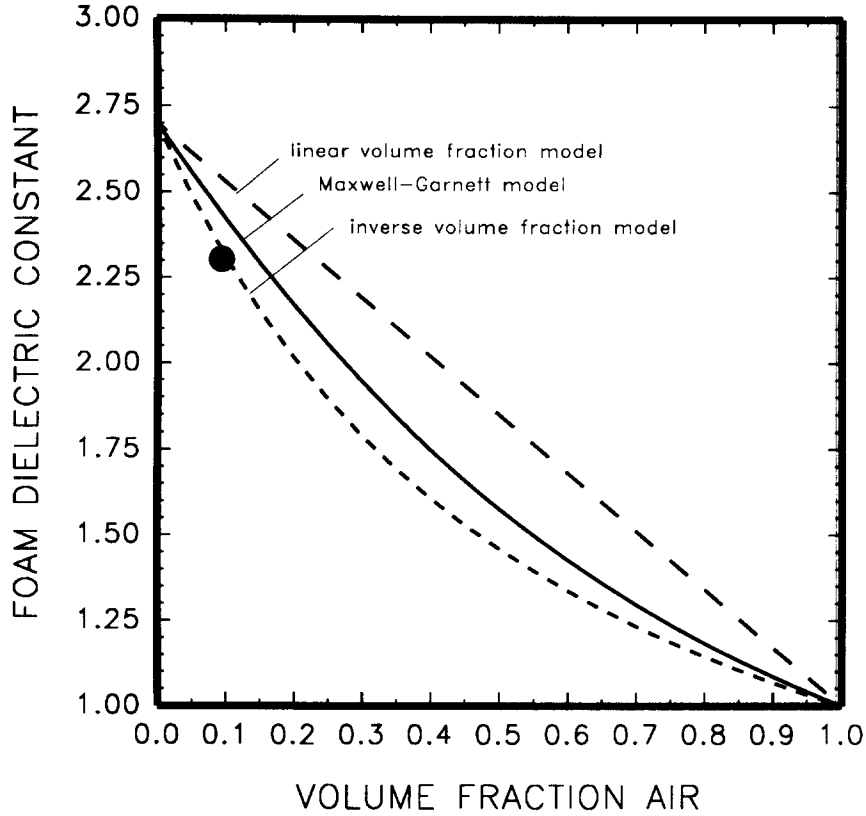

Figure 11 Calculated foam dielectric constant as a function of the volume fraction of air

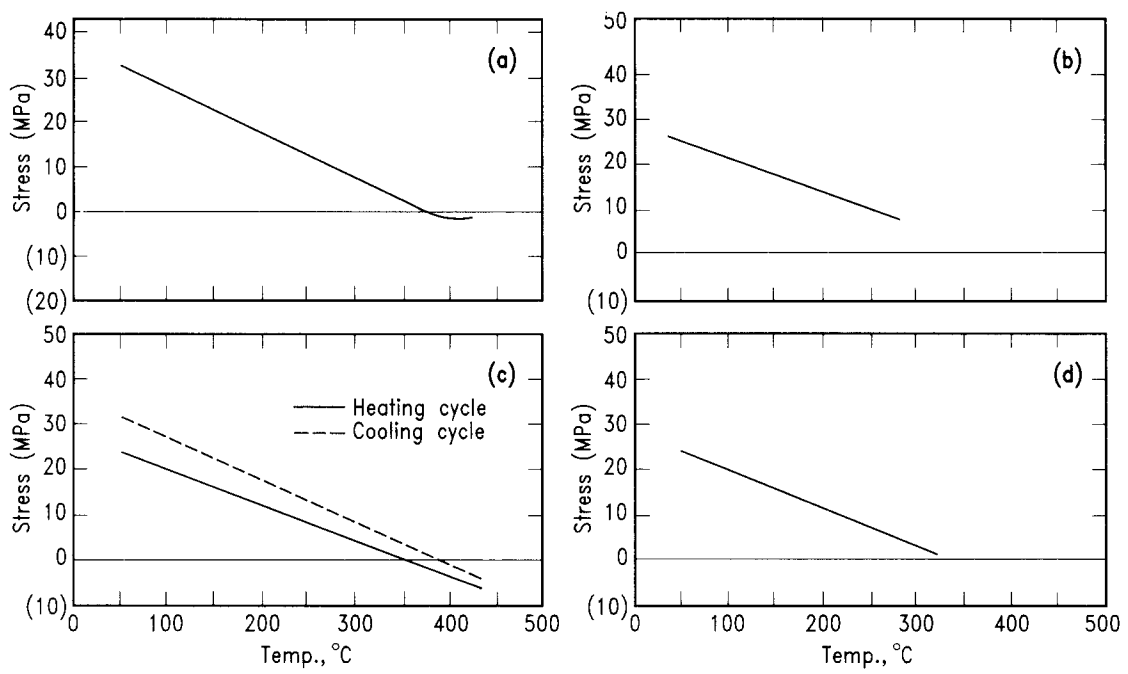

Figure 12 Stress *versus* temperature plots for: (a) PPQ; (b) foamed copolymer 2; (c) foamed copolymer 2 heated to 400°C; (d) foamed copolymer 5

molecular orientation and thermal expansion coefficient. The generation of a foam reduces the modulus according to the volume fraction of voids, while the thermal expansion coefficient remains essentially the same. Thus, the stress should, in principle, drop with reduction in the modulus. *Figure 12* shows the stress *versus* temperature plots for PPQ (*Figure 12a*), the foamed copolymer 2 which was heated to 275°C (*Figure 12b*), the foamed copolymer 2 heated to 400°C (*Figure 12c*) and the foamed copolymer 5 (*Figure 12d*). PPQ heated to just above T_g has moderate residual thermal stress from thermal cycling (~40 MPa). As expected, both the foamed copolymers 2 and 5 show lower residual stress values upon cooling from 275°C. However, heating copolymer 2 above the T_g at 400°C (for 1 h) to collapse the foam, produced higher residual thermal stress upon cooling. Although it has been reported that the ultimate strength of polymeric foams is somewhat diminished, advantages in residual thermal stress were realized by the generation of the nanofoam.

REFERENCES

1 Tummala, R. R. and Rymaszewski, E. J. 'Microelectronics Packaging Handbook', Van Nostrand Reinhold, New York, 1989, Ch. 1
2 Russell, T. P. *J. Polym. Sci., Polym. Phys. Edn* 1986, **22**, 1105
3 Takahashi, N., Yoon, D. Y. and Parrish, W. *Macromolecules* 1984, **17**, 2583
4 Boese, D., Herminghaus, S., Yoon, D. Y., Swalen, J. D. and Rabolt, J. F. *Mater. Res. Soc. Symp. Ser.* 1991, **227**, 379
5 Haider, M., Chenevey, E., Vora, R. H., Cooper, W., Glick, M. and Jaffe, M. *Mater. Res. Soc. Symp. Proc.* 1991, **227**, 35
6 Critchley, J. S., Gratan, P. A., White, M. A. and Pippett, J. S. *J. Polym. Sci. A-1* 1972, **10**, 1789
7 Harris, F. W., Hsu, S. L. C., Lee, C. J., Lee, B. S., Arnold, F. and Cheng, S. Z. D. *Mater. Res. Soc. Symp. Proc.* 1991, **227**, 3
8 Sasaki, S., Matsuora, T., Nishi, S. and Ando, S. *Mater. Res. Soc. Symp. Proc.* 1991, **227**, 49
9 Labadie, J., Sanchez, M., Cheng, Y. Y. and Hedrick, J. *Mater. Res. Soc. Symp. Proc.* 1991, **227**, 43
10 Gaghani, J. and Supkis, D. E. *Acta Astronaut.* 1980, **7**, 653
11 Smearing, R. W. and Floryan, D. C. US Patent 4.543.365 to General Electric, 1985
12 Krutchen, C. M. and Wu, P. US Patent 4.535.100 to Mobil Oil, 1985
13 Hoki, T. and Matsuki, Y. European Patent 186308 to Asahi Chem, 1986
14 Meyers, R. A. *J. Polym. Sci. A-1* 1969, **7**, 2757
15 Carleton, P. S., Farrissey, W. J. and Rose, J. S. *J. Appl. Polym. Sci.* 1972, **16**, 2983
16 Alvino, W. M. and Edelman, L. E. *J. Appl. Polym. Sci.* 1975, **19**, 2961
17 Farrissey, W. J., Rose, J. S. and Carleton, P. S. *J. Appl. Polym. Sci.* 1970, **14**, 1093
18 Riccitiello, S. R. and Sawako, P. M. US Patent 4.177.333 to NASA, 1979
19 Hamermesh, C. L., Hogenson, P. A., Tun, C. Y., Sawako, P. M. and Riccitiello, R. 11th National SAMPE Technical Conference 1979, p. 574
20 Gagliai, J. US Patent 4.241.193 to International Harvester, 1980
21 Lee, R., Okey, D. W. and Ferro, G. A. US Patent 4.535.099 to IMI-Tech Corp., 1985
22 Sillion, B., Senneron, M. and Parroun, G. US Patent 5036111
23 Alberino, L. M. *Cell. Plast. Conf.* 1976, **4**, 1
24 Narkis, M., Paterman, M., Boneh, H. and Kenig, S. *Polym. Eng. Sci.* 1982, **22** (7), 417
25 McWhirter, R. J. *Energy Res. Abs.* 1981, **6**, 2627
26 McIlroy, H. M. *Energy Res. Abs.* 1977, **2**, 3469
27 Gagliani, J., Lee, R., Sorathin, U. A. K. and Wilcoxson, A. L. *Sci. Tech. Aerosp. Rep.* 1980, **18**, 37
28 Gagliani, J. and Supkis, D. E. *Adv. Astronaut. Sci.* 1979, **38**, 193
29 Patel, N. M., Yoo, Y. T., Soner, K., McGrath, J. E., Moy, C. H. and Prine, R. B. Proceedings of the 34th International SAMPE Conference, 1989
30 Labadie, J. and Hedrick, J. *J. Polym. Sci., Polym. Chem. Edn* in press
31 Hergenrother, P. M. and Levine, H. H. *J. Polym. Sci., Polym. Chem. Edn* 1967, **5**, 1453
32 Hergenrother, P. M. *J. Macromol. Sci., Rev. Macromol. Chem.* 1971, **C6**, 1
33 Hergenrother, P. M. *J. Appl. Polym. Sci.* 1974, **18**, 1779
34 Debye, P. and Beuche, A. M. *J. Appl. Phys.* 1940, **20**, 518
35 Debye, P., Anderson, H. R. and Brumberger, H. *J. Appl. Phys.* 1957, **28**, 679
36 Kratky, O. *J. Pure Appl. Chem.* 1966, **12**, 483